



# Analysing the acoustic performance of a nearly-enclosed noise barrier using scale model experiments and a 2.5-D BEM approach

Qiutong Li, Denis Duhamel, Yanyun Luo, Honore Yin

## ► To cite this version:

Qiutong Li, Denis Duhamel, Yanyun Luo, Honore Yin. Analysing the acoustic performance of a nearly-enclosed noise barrier using scale model experiments and a 2.5-D BEM approach. *Applied Acoustics*, 2020, 158, pp.107079. 10.1016/j.apacoust.2019.107079 . hal-02914702

**HAL Id: hal-02914702**

**<https://hal.science/hal-02914702>**

Submitted on 12 Aug 2020

**HAL** is a multi-disciplinary open access archive for the deposit and dissemination of scientific research documents, whether they are published or not. The documents may come from teaching and research institutions in France or abroad, or from public or private research centers.

L'archive ouverte pluridisciplinaire **HAL**, est destinée au dépôt et à la diffusion de documents scientifiques de niveau recherche, publiés ou non, émanant des établissements d'enseignement et de recherche français ou étrangers, des laboratoires publics ou privés.

# Analyzing acoustic performance of a nearly-enclosed noise barrier using scale experiments and a 2.5-D BEM approach

Qitong Li, Denis Duhamel, Yanyun Luo, Honore Yin

---

## Abstract

This paper describes scale modelling method to measure the acoustic performance of a nearly-enclosed barrier and corresponding predictions using an existing 2.5-D Boundary Element Method(BEM) program. Preliminary investigation results show the deterioration in performance of a nearly-enclosed barrier due to the resonance effect that led to high pressure levels radiating into the surroundings via the topped opening. Absorptive material added to the inner surface of the barrier can effectively improve this phenomenon. Measurements on one-twentieth scale model of barriers, viaducts and vehicle structures were carried out outdoors under controlled conditions. The measured results show the transmission loss of transparent panels on the top were not adequate to make the measured results as high as the predictions. A modified scale model, by coating all the surfaces with rubber, was remeasured. The results from retested tests and calculations were in good agreement each other, which indicate that the 2.5-D BEM code can provide a reliable description of the acoustic performance of a nearly-enclosed barrier. Then the program was able to be employed into the investigation of barrier performance on every area with different acoustic features in the surrounding environment. As expected, the attenuation of the nearly-enclosed barrier averaged around 15 dB in the near field and around 10 dB in the far field. The number effect of incoherent point sources on the performance is discussed as well for the study of railway traffic noise. The increased number of incoherent point sources can result in smoother and lower attenuations for the whole sound field.

*Keywords:* Enclosed noise barrier, scale model measurement, BEM

---

## 1. Introduction

In general, noise barriers are built on the side of viaducts to reduce urban railway traffic noise pollution. The associated acoustic performance is thought to depend largely on their height and the relative distance between the source, the barrier and receiver positions[1]. There is almost no change for the latter since the predominant source for urban railway traffic is located on the place of wheel-rail interaction, and the barrier position, varying with changes of width of the viaduct, remains basically unchanged. To improve the performance devices installed on the top of the barrier are sometimes introduced instead of the height increase. Among all the barriers on the market, enclosed types are common solutions to improve the most. LI. et al.[2] studied on the noise reduction of semi- or fully-enclosed barriers of high speed railways using the full-scale modelling. The results showed that the attenuation of fully-enclosed metal noise barrier with composite sound absorption plates was up to 25 dB(A) at 7.5m distance from the track central line. However, the barrier cannot be fully-enclosed when consider the fire safety. Since the space inside an enclosed barrier is very small when a train passes by, an opening, commonly with a two-meter height, is designed on the top so that smoke can be emitted when fire occurs. In the present study this kind of barrier is called a nearly-enclosed barrier, one of the prototypes depicted in Figure 1. The two arched parts on the top are made of 6.5-mm-thick PC panels that allows in natural light and to reduce limitation of drivers' view[3]. One of the important issues is the sufficiency of the sound insulation property of such material that is required to achieve suitable acoustical performance.

Another for that is the multiple reflections between two axisymmetric parts and between the extremely high barrier and the vehicle surface that significantly degrade barrier performance. Watts[4] found a reflecting wall with a 2m height fixed on the source side could result in a reduction of 4 dB(A) in the insertion loss of a sound barrier of the same height. More seriously in our study, the acoustical domain bounded by a nearly-enclosed barrier can be considered as a room with a door or an open duct, and then the sound field within such domain can be dominated by acoustic resonance. Under the influence of this effect high pressure amplitudes may be observed at the resonant frequencies leading to the significant degradation of barrier performance. In the parametric investigation of the performance of multiple edge highway noise barriers, D.J. Oldham and C.A. Egan[5] observed the

acoustic resonance in the air in the gap between an edge and the barrier face resulting in the negative relative insertion loss for the configurations involving reflective edges located on the source side of the barrier. In parallel with this development, Yang et al.[6] firstly proposed the resonance effect of the trapped modes to explain the deterioration in performance of a conventional barrier due to the reflecting surface. To solve the multiple reflections and the peak sound pressures governed by resonance, a tilted barrier was proposed[7, 8] as a solution with a slope of ten degrees gaining the best profit and a wave-trapping barrier was proposed[6] effectively in reducing the deterioration at peak frequencies. Furthermore, absorptive materials were employed on the surface of reflective barrier near the source being able to reduce the deterioration with highly efficiency[9].

A number of studies have made clear the importance of "T", "Y" and other top devices in improving the diffraction reduction of barriers but there is little research as a specific guidance that can be applied to the problems discussed in this paper. Thus the objective of this research is to analyze acoustic performance of a nearly-enclosed barrier using numerical and experimental method. An existing 2.5-D BEM program was used to characterise the acoustic performance of a nearly-enclosed barrier on every area with different acoustic features in the surrounding environment. Its reliability was validated by comparing predictions with measured results from scale model tests. The scale modelling technique is more efficient and more accurate to not only investigate barrier performance, but also to realize the effect of related parameters on the acoustic performance. By using scale experiments and 2.5-D BEM approach the efficiency of noise reduction of constructed panels and the number effect of incoherent point source are also studied.

Section 1 of this paper briefly introduces a nearly-enclosed barrier commonly applied on the city viaduct railway traffic system and some relevant issues need to be resolved. Section 2 presents a 2.5-D BEM model obtained from a real prototype. The resonance effect of acoustic modes on barrier performance is also described by a preliminary investigation in this section. Section 3 validates the numerical model by a series of scale measurements. As a result of the measured results much lower than those predictions, the sound insulation property of transparent material is discussed in this section. Then a series of remeasurement on the modified model is described and the results give confidence in the subsequent predictions. Section 4 predicts acoustic performance of a nearly-enclosed barrier by using 2.5-D BEM modelling. The attenuation of barrier located at several receiver positions



76 in the near and far field comparing different source types are discussed in  
77 detail, and all the predicted results are summarized. Section 5 gives a brief  
78 conclusion in this paper.

## 79 **2. 2.5-D Boundary element modelling**

80 Based on the direct formulation of Boundary Element Method(BEM), the  
81 2-D, 2.5-D and 3-D BEM numerical methods were developed and detailed in  
82 [10–15]. In the 2-D numerical simulation, a 2-D point source is commonly  
83 approximated as an infinite coherent line source in three dimensions; the bar-  
84 rier and other obstacles are defined with the cross-section remaining constant  
85 and infinite along a direction perpendicular to the section plane. 2.5-D BEM  
86 method gives a chance to allow the use of other sources like a point source or  
87 an incoherent line source but remain the geometrical characteristics of all the  
88 obstacles. DUHAMEL[14] compared these three source types and figured out  
89 that the results predicted for a coherent line source were basically equivalent  
90 to that for a point source while incoherent line source showed considerable  
91 difference in frequency domain. P. Jean et al.[15] emphasized the importance  
92 of source type in the numerical modelling based on the calculation of 2.5-D  
93 BEM approach. They found the attenuation of conventional noise barriers  
94 for a coherent line source was much higher than that for an incoherent line  
95 source. Considering that the road/railway traffic noise is commonly assumed  
96 as one or more than one incoherent line sources[3, 12, 15, 16], using 2-D  
97 BEM modelling with coherent line sources must result in the overestimation  
98 of barrier performance. As a consequence, it was decided to carry out the  
99 calculations with a 2.5-D model using different numbers of incoherent point  
100 sources.

101 To validate a model nearly-enclosed barrier in three dimensions by BEM  
102 requires a certain amount of time for the high complexity of the computing  
103 process due to the complex geometry of the barrier. Based on the numerical  
104 method proposed in [14], a 2.5-D existing program was used to carry out 3-D  
105 boundary element calculations from solutions of problems defined in two-  
106 dimensional domains outside the associated cross-section. By using BEM to  
107 solve the acoustic problems in two-dimensional domains, the efficiency of the  
108 calculation is considerably improved. At the beginning of 2.5-D calculation,  
109 the source is assumed as coherent line source perpendicular to the page plane  
110 at first, which maintains the two-dimensional nature of the model. Subse-  
111 quently by Fourier-like transformation the sound pressure fields created by

the coherent line source for the whole frequency spectrum will be converted into those radiated by a point source in three dimensions. The third position of the point source, defined relative to the plane where the two-dimensional calculation has been done, was considered in the existing program as well. Hence it was possible to calculate sound pressure for a line of such incoherent point sources.

The 2.5-D model of a nearly-enclosed barrier was obtained from the real prototype located on the viaduct of Metro 1 in Ningbo city, China, as shown in Figure 1. The noise barrier and the viaduct were assumed infinite uniform in construction along their length. In reality the barriers are installed on the viaducts so that there is no gap between the barriers and viaducts. However, on the basis of the BEM principle the distance between these two independent boundaries is at least larger than the element size[17]. Thus, this requires the geometry removal of the connections between them and therefore the boundaries of the viaduct and the barrier were integrated as a whole. These changes in the model are illustrated in Figure 2. The shape of vehicle source was simplified as a rectangle based on measurements of the stock Type B of China Railway Rolling Stock. The height assumed was 3.7 m and the width was 2.8m. It can be seen from Figure 2 that the source was placed at the outside wheel-rail interaction position. All the boundaries of the vehicle structure were made acoustically rigid. Taking into account reflections from the ground, the reflection from the image source symmetric to the source was also introduced into the model and the height of the viaduct above ground was 10 m.

To improve the precision requirement, the size of quadratic order ele-

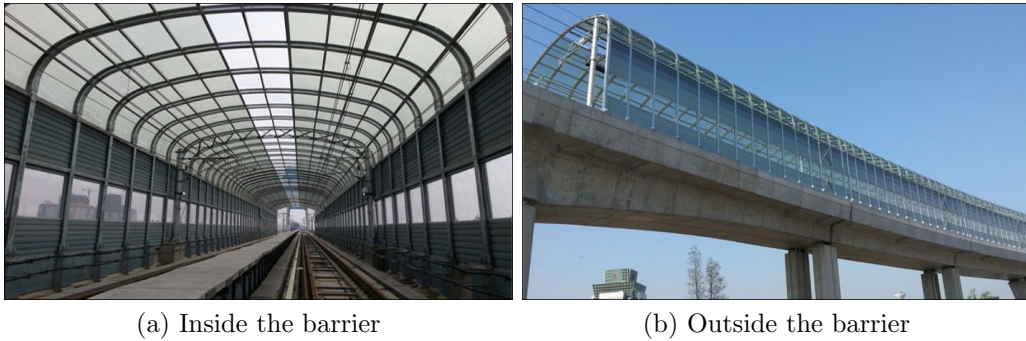


Figure 1: A prototype of the nearly-enclosed barrier located in Ningbo, China

ment was defined as one tenth of the minimum wavelength. Furthermore,

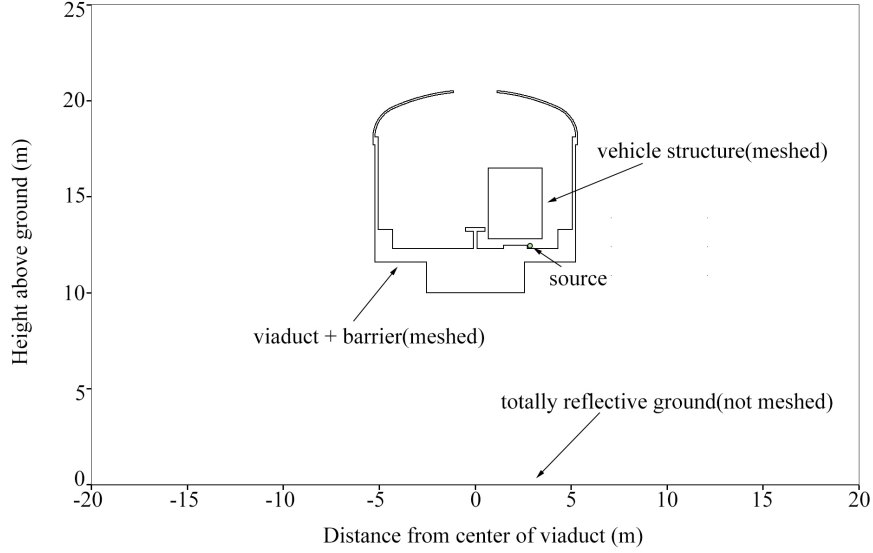


Figure 2: Numerical model for nearly-enclosed barriers on urban railway viaducts solved by 2.5-D BEM program

numerical predictions were calculated at third octave frequencies from 50 Hz to 1000 Hz.

A preliminary investigation was performed with the BEM predictions to understand the mechanism of the multiple reflections inside a nearly-enclosed barrier. In Figure 3, the blue areas represent pressure levels for the coherent line source as a function of frequency, fluctuating violently with a huge number of sharp-pointed peaks. Although the peak value decreases with increasing of frequency, with the rise in the number these peaks progressively dominate the sound pressure at a given receiver. Similar trends can be observed as well for the one-point source by the green areas, and these peaks retain their relative high levels at the similar frequencies. These peak levels would directly cause the deterioration of barrier performance that could not be ignored. According to the principle of resonance modes as referred in Section 1, several acoustic modes of the air cavity inside the barrier fully enclosed by Neumann boundaries, which corresponds the sound pressure level distribution at peak frequencies marked by red circles in Figure 3, are depicted. Figure 4&5 shows the 2D BEM results and the FEM acoustic modes. Good agreements on the contours and the peak frequency values are easily observable, which means these peak levels in the frequency domain were the

157 result of the resonance effect of the open-air cavity. Besides that, it is signifi-  
 158 cant to note that the topped opening was not able to eliminate the resonance  
 159 effect, but also leak high pressure levels into the surrounding region, thereby  
 160 impacting seriously the noise reduction ability of the nearly-enclosed barrier.  
 161 If some absorptive treatments are further added to the inner surface of the  
 barrier, it is effective to improve the performance.

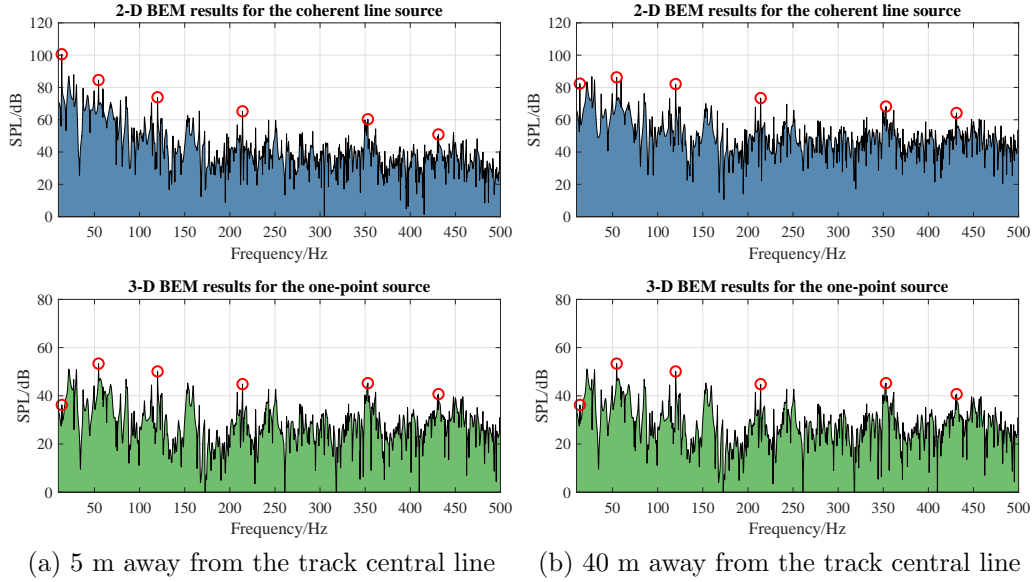


Figure 3: The spectrum of sound pressure levels in the near and far field governed by the nearly-enclosed barrier(the receivers are positioned at the height of source)

162

### 163 3. Scale model measurement

164 To validate the predicted results for a nearly-enclosed barrier, the method  
 165 of acoustic scale modelling was introduced. Scale model measurement has  
 166 strict request to measurement environment. The test site has to be delib-  
 167 erately left as open as possible in order to emphasize the diffraction sound  
 168 generated by the barrier model and prevent reflection sound caused by any  
 169 reflecting surface close to the model from affecting the measured results. The  
 170 site was finally selected as shown in Figure 6(a), which fully met the require-  
 171 ment specified previously. Considering the site limitations, the scale of the  
 172 barrier model in our case was determined as 1:20.

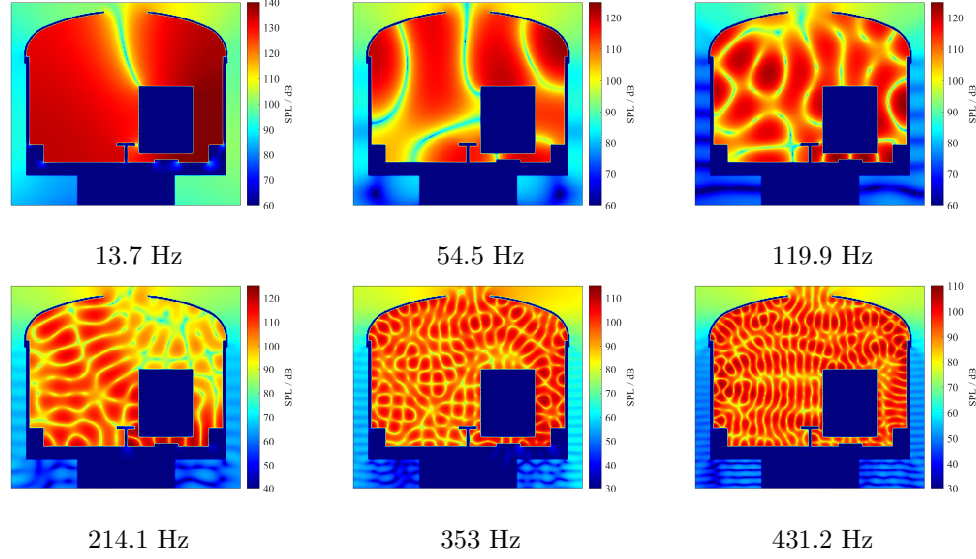


Figure 4: Pressure level distribution inside the barrier of 2-D BEM model

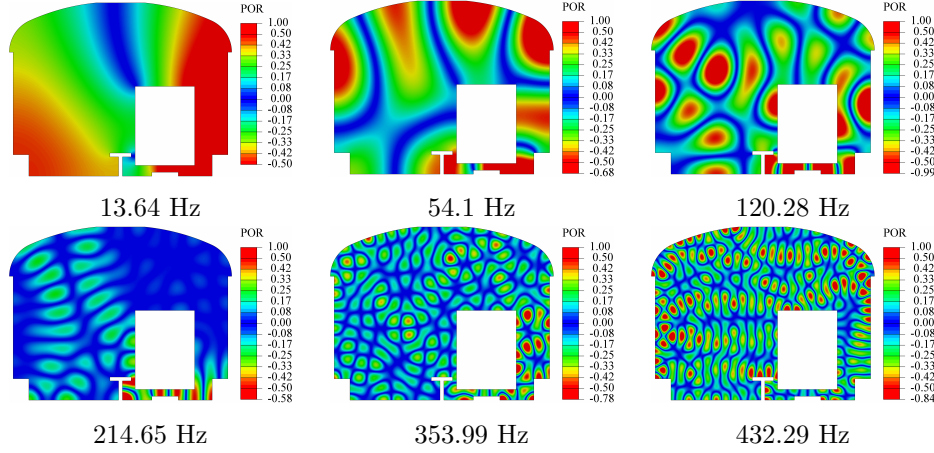


Figure 5: Several acoustic modes of the air cavity fully enclosed by the Neumann boundaries inside the 2.5-D BEM model of the nearly-enclosed barrier

### 173 3.1. Measurement apparatus

174 Generally loudspeakers and microphones are the indispensable transduc-  
 175 ers in an acoustic experiment. In order to send the electrical audio signal to  
 176 the loudspeaker and receive it from the microphone synchronously, a collec-  
 177 tion of electronic apparatus was prepared. Miniature speakers with the size

178 of less than  $1\text{ mm}^3$  were chosen in our study since the space where the speaker  
 179 located was less than  $10\text{ cm}^3$  (approximately the size of an eraser). Commonly  
 180 a normal-sized loudspeaker has a diameter of at least  $30\text{ mm}$ , which is too  
 181 large to be placed inside this model. The spectrum of the speaker was mea-  
 182 sured at several angles. It was found to be omni-directional when towards  
 183 to the microphone. During the formal measurement for each test several  
 184 employed loudspeakers emitted simultaneously white noise with one of the  
 185 third octave spectrum from the signal output module. For these miniature  
 186 loudspeakers the amplifiers and the power supply were selected accordingly.  
 187 On the other hand, the highly sensitive B&K microphones 4189-A-021 sat-  
 188 isfy the requirements of such high-precision, free-field measurement. They  
 189 were powered from the supply offered by the DAQ signal output module.  
 190 All the electronic apparatus were put under the model above ground, which  
 191 did not appear in the transmitting path between the loudspeakers and the  
 192 microphones affecting the measured results.

193 A VI project was designed in the LabVIEW development environment  
 194 to transmit\receive electric signals. Figure 6(b) illustrates the signal flow  
 195 graph of the measurement. It can be seen clearly that the original source  
 196 signal was generated by the VI project from the laptop, transmitting to the  
 197 output module, via the amplifier to the loudspeaker. In the meantime, sound  
 198 pressure signal was received and preamplified by the microphone, via the in-  
 199 put module back to the laptop, finally saved by the VI project. It is worth  
 200 emphasizing that the VI project did not only play a role as a signal generator  
 201 for activating the loudspeaker, it also undertook that of receiving, saving and  
 analysing the signals from the receivers.

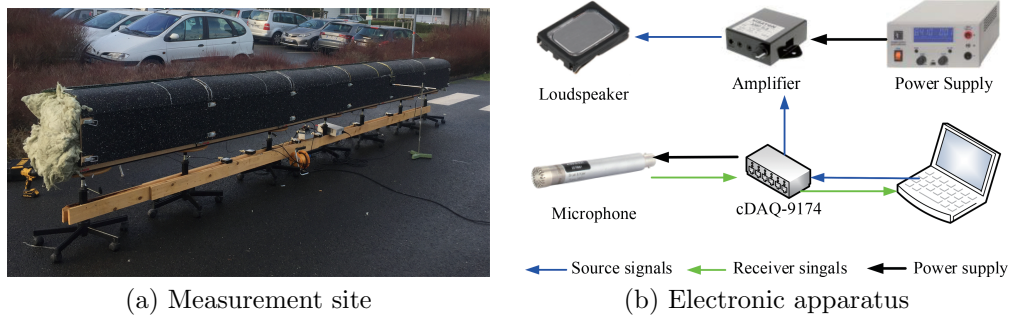


Figure 6: Scale measurement preparation

### 203 3.2. Scale model measurements

204 All barriers used in the experiment were a twentieth of the full scale nu-  
 205 merical models. It was necessary to build simplified models for the complex  
 206 structure so that sound diffraction towards the barrier would dominate at-  
 207 tenuation measurements, facilitating comparison with the predictions from  
 208 the BEM model which being 2.5-D in the space with infinitely long barriers.  
 209 The tests were made in six configurations, of which the cross-sections were  
 210 shown in Figure 7,

- 211 • Tests with viaducts and nearly-enclosed barriers(Figure 7(a1)(a2)).
- 212 • Tests with viaducts and double-straight barriers(Figure 7(b1)(b2)).
- 213 • Tests with viaducts(Figure 7(c1)(c2)).

214 The blue parts represent PC panels with a thickness of 5 mm and the brown  
 215 parts are 9-mm-thick assembled wood planks. Tests were made with and  
 216 without vehicle structures which were one twentieth the practicable 3.7x2.8  
 217 m<sup>2</sup> in full scale.

218 The 1:20 scale model was an assembly of six sections the length of each  
 219 section being defined as 1 m since the metro vehicle is 19 m long and each  
 220 train has six vehicles in reality. However, sound transmitting over the two  
 221 ends of the model to the microphone must affect sound pressure level at the  
 222 receivers. In order to reduce the end effect as much as possible, both barrier  
 223 ends were filled with mineral wool to absorb sound(shown in Figure 6(a)).

224 There were twelve loudspeakers arrayed along the length of the six-section  
 225 model. Each section of the model had two sources placed exactly at the po-  
 226 sition of each vehicle wheel in reality. The position in the cross section was  
 227 close to the location of the wheel-rail interaction, in accord with that of the  
 228 point source in the 2.5-D BEM model. A time-history signal of white noise  
 229 was taken as the input of the sound source to the loudspeaker. Each of  
 230 the signals was individually coherent but mutually incoherent to the others.  
 231 Figure 8 and Table 1 present these co-ordinates and the numbers of the loud-  
 232 speakers. The sampling position for the microphone was placed exactly at  
 233 the cross-section where the 7th loudspeaker positioned.

234 Two sets of tests were taken to determine the third octave sound pressure  
 235 levels outside the barriers. Tests were completed with the viaduct but with-  
 236 out barriers(Figure 7(c1)(c2)) so that the attenuation could be calculated  
 237 as the difference between the sound pressures measured in the presence and  
 238 absence of barriers. Tests with viaducts and double-straight barriers(Figure

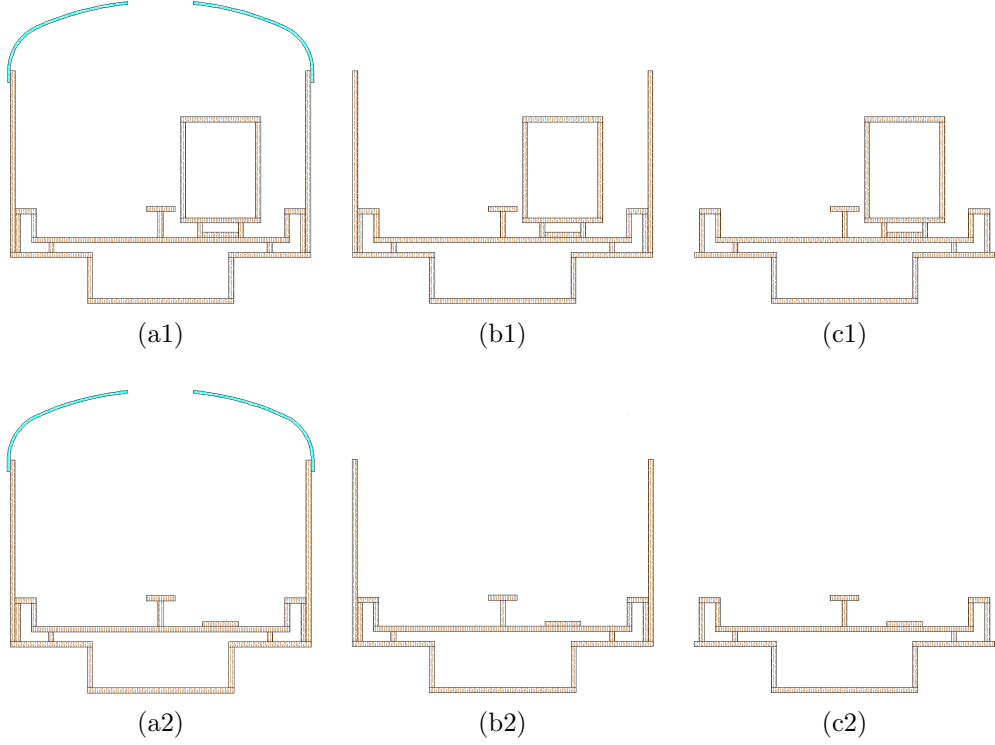


Figure 7: All the configurations of tested models. The upper row shows the models with vehicle structures and the lower row shows the models without vehicle structures.

239 7(b1)(b2)) were completed as well in order to understand the sound insula-  
 240 tion property of the PC panels. In addition, the attenuations at the third  
 241 octave band frequency from 1000 Hz to 20 kHz were tested to validate the  
 2.5-D BEM predictions from 50 Hz to 1000 Hz.

Table 1: Positions of loudspeakers and microphone in three co-ordinates(cm)

Loudspeaker			Microphone		
$X_s$	$Y_s$	$Z_{si}(i=1,2,\dots,12)$	$X_r$	$Y_r$	$Z_r$
3.6	0.5	-296.7, -233.7, -197.8, -134.8, -98.9, -35.9, 0, 63.0, 98.9, 161.9, 197.8, 260.8	25.6	19.0	0



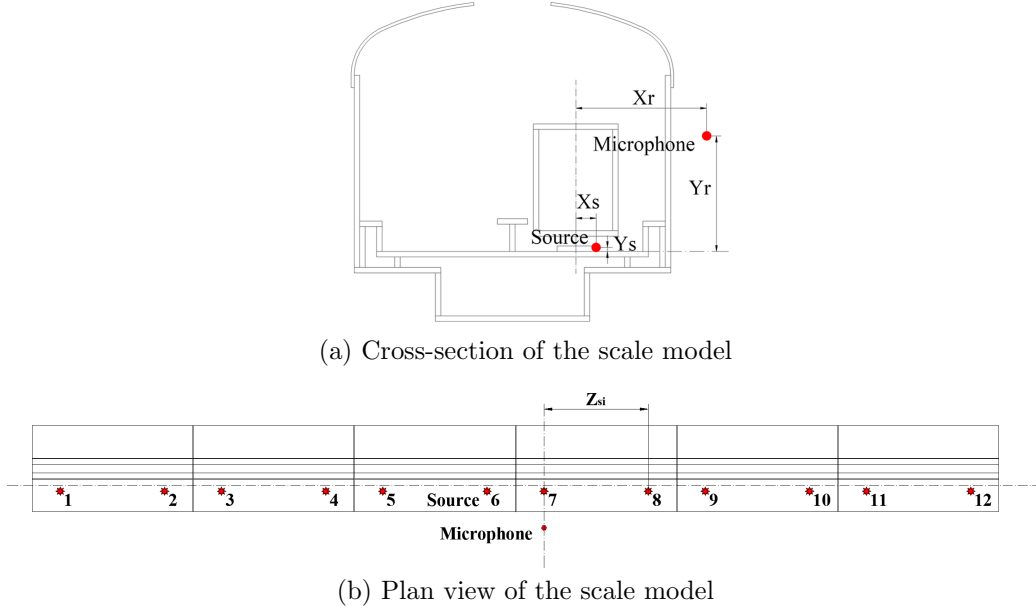


Figure 8: Experimental arrangement for the nearly-enclosed scale barrier

### 3.3. Comparisons with BEM predictions

Predictions were carried out for the nearly-enclosed and double-straight barriers using the 2.5-D BEM program. The number of the incoherent point sources defined was one(the 7th) at first. Subsequently when numerical predictions were validated by measured results, the number would add up to four(the 5th, 6th, 7th and 8th) and finally to all twelve.

For one point source facing the microphone, Figure 9(a) shows plots of measured and predicted attenuations by the third octave band in the case of the double-straight barriers on the viaduct with and without vehicles. The predicted third octave source spectra was adjusted in the analysis so that the effective source spectra used in the BEM and scale models were identical (note that further frequencies in Section 3 will be given in the scale 1:20 for the sake of clarity). It is clear that as expected there is good agreement for each comparison between the measured results and those predicted by the 2.5-D BEM approach. The small deviation between the measured and predicted results is normal and permissible due to the non-idealised point source used for measurements.

Figure 9(b) shows the compared results for the nearly-enclosed barrier

on the viaduct. It is worth noting that the measured attenuations are much lower than those predictions regardless of the vehicle structures present, especially for high frequencies. And these measured results are as high as those measured for the double-straight type. With the finding of these significant differences between the measured and predicted results for the nearly-enclosed barrier, a strong argument can be made that the PC panels on the top were not considered to be acoustically rigid. This finding might be due to the sound insulation properties of the PC panels and wood planks which were not sufficiently high to reduce sound transmission through the nearly-enclosed barrier.

### 3.4. Sound insulation problem

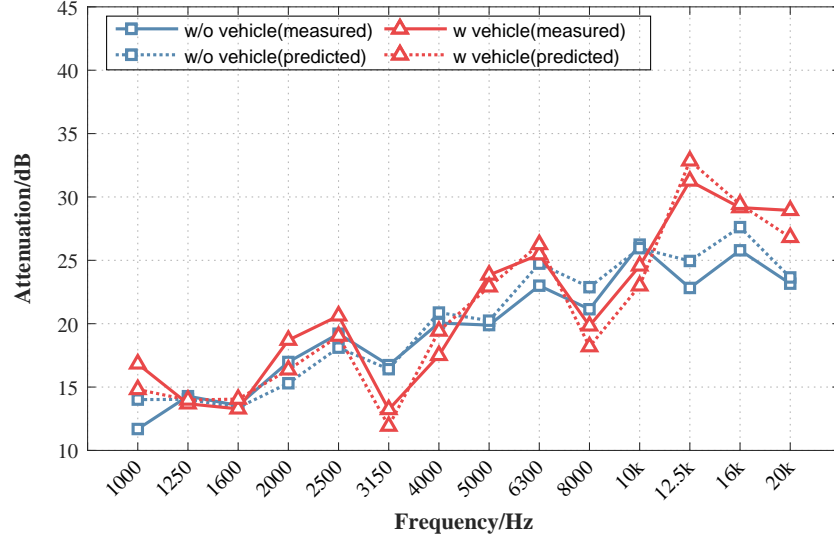
The sound insulation properties of material is usually evaluated by an acoustic physical term [18] i.e., sound transmission loss known as TL which is defined as 20 times the logarithm of the ratio of the acoustic pressure associated with the incident wave and that of the transmitted wave.

In terms of energy transfer, attenuation of the sound barrier (also known as Insertion Loss) depends precisely on the energy distribution of sound diffraction over the top, transmission through the barrier and reflection bounced off its surface. Considering the effect of ground absorption, the practical attenuation of the sound barrier is given as,

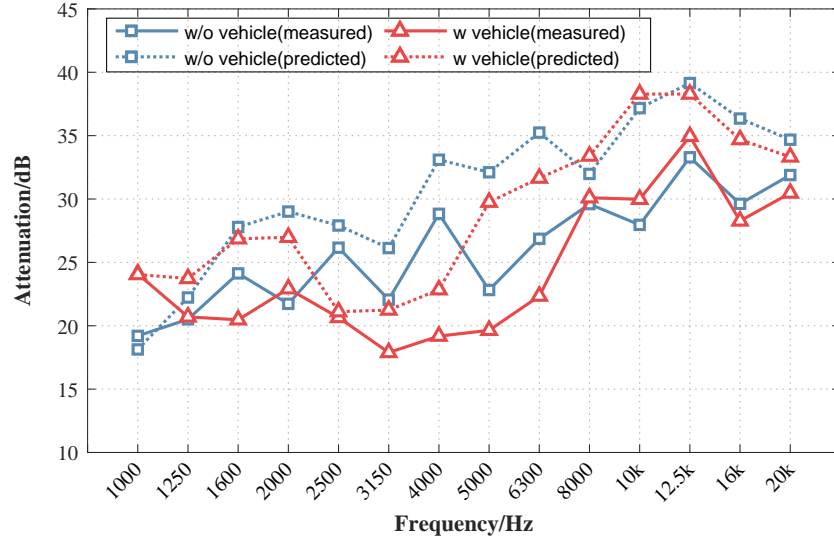
$$IL = A_d - C_t - C_r - C_G \quad (1)$$

where  $A_d$  denotes diffraction attenuation of the barrier top and side edges, which is the most important physical phenomenon in the noise reduction process.  $C_t$  is the correction value for sound transmission through the barrier,  $C_r$  is the correction for the sound reflection bounce off the barrier and  $C_G$  is the correction for ground absorption.

Typically, the diffraction attenuation  $A_d$  is much lower than the TL of high-density materials employed in the construction of the barrier, at least 10 dB. And in such case the correction for sound transmission  $C_t$  is negligible in the overall performance of the barrier. However, the predicted attenuations of the nearly-enclosed barrier have been found greatly higher than 20 dB over the frequency range of 1000 Hz-20 kHz shown in Figure 9(b). These values might be extremely close to those for the TLs of the employed materials so that the correction  $C_t$  could not be ignored in the calculation of the insertion loss. According to Eq (1) the measured attenuations were therefore lower



(a) Double-straight barrier on the viaduct



(b) Nearly-enclosed barrier on the viaduct

Figure 9: Measured and predicted attenuations for the model(a) double-straight barrier(Figure 7(b1)(b2)); (b) nearly-enclosed barrier(Figure 7(a1)(a2))

295 than our expectations.

296 Since the barrier attenuation is frequency dependent and so is the impact

297 of transmission loss, to better understand their relationship, the compar-  
 298 isons for high frequencies between the predicted attenuations for the nearly-  
 299 enclosed and the double-straight barrier and the measured TLs for the PC  
 300 panels are illustrated in Figure 10. The blue and red curves without symbols  
 301 represent the TLs for PC panels measured by Woo-Mi Lee et al.[19] with a  
 302 thickness of 4 mm and 8 mm, respectively. On account of the thickness of  
 303 the PC panel in our test being 5 mm, its TL curve must be sensibly lying in  
 304 the region between these two curves. At the frequency higher than 4000 Hz,  
 305 the value of TL theoretically tends to increase 6 dB per octave band. As a  
 306 consequence, the approximated transmission loss of the employed PC panels  
 307 in our test was estimated reasonably for each third-octave band of interest  
 308 according to the discussion above, which is represented by the green dotted  
 309 line shown in Figure 10. The blue and red curves with rectangular symbols  
 310 in Figure 10 represent the predicted attenuations for the nearly-enclosed and  
 311 double-straight barrier, respectively. It is obvious that at frequencies from  
 312 1000 Hz to 2000 Hz and from 4000 Hz to 12.5 kHz the approximated TLs  
 313 are quite close to the predicted attenuations for the nearly-enclosed type,  
 314 but much higher than those for the double-straight type by at least 10 dB.  
 315 Hence the correction term of sound transmission must be taken into account  
 316 and in such case the boundary condition of two arched PC panels cannot  
 317 be considered as totally reflected in the BEM model for the nearly-enclosed  
 318 barrier. Therefore, we can conclude that the insufficient insulation property  
 319 of the PC panels must be the foremost reason for the considerable differ-  
 320 ences between the predicted and measured results mentioned previously for  
 321 the nearly-enclosed barrier.

322 To improve the sound insulation property of the arched parts for the  
 323 nearly-enclosed barrier so that better measured attenuations could be tested,  
 324 a kind of material that provides good sound insulation as well as flexibility  
 325 was needed. The transmission loss of a typical single-layer material is theo-  
 326 retically divided into three distinct performance regions developed from the  
 327 frequency range: I. stiffness and resonance region, II. mass region and III.  
 328 coincidence region. Region I typically ranges below 200 Hz[20] where the TL  
 329 is controlled by the stiffness and the resonance frequency of the material. In  
 330 Region II the relationship between TL and frequency is mainly controlled by  
 331 the mass of material, which is known as the mass law: each time the mass  
 332 is doubled the TL increases 6 dB. This law continues to meet the critical  
 333 frequency  $f_c$  at which sound waves incidents are able to efficiently transfer  
 334 energy to the panel. This phenomenon is called the "coincident effect" which

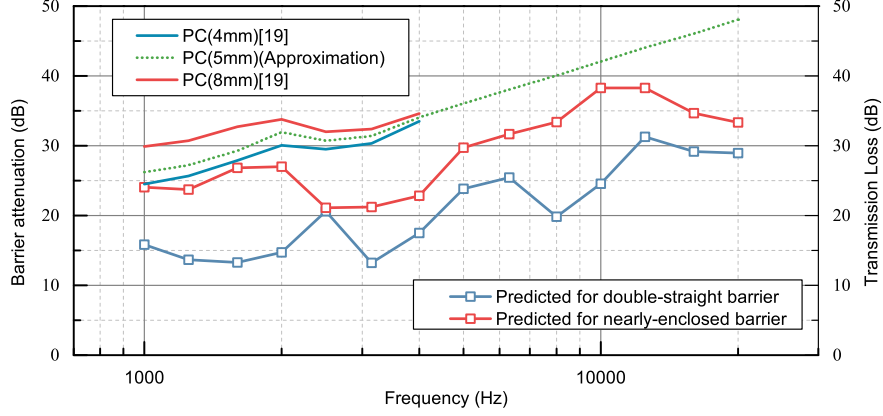


Figure 10: Comparison between the predicted attenuations of barriers and the TLs of PC panels

severely influences the sound insulation performance of the material. The critical frequency for a single-layer isotropic homogenous material is defined as,

$$f_c = \frac{c^2}{2\pi t} \sqrt{\frac{12\rho_m(1-\sigma^2)}{E}} \quad (2)$$

where  $c$  denotes sound speed,  $t$  is the thickness of material and  $\rho_m$  is mass of the panel per unit surface area.  $E$  and  $\sigma$  are Young's modulus and Poisson's ratio of the material, respectively.

Taking for instance the 5-mm-thick PC panel with an average density of  $1.2 \text{ g/cm}^3$  employed in the scale measurement, the TL fluctuates violently in Region I, then increases by 6 dB per octave in Region II and suddenly declines significantly when approaching critical frequency. At higher frequencies the TL continues to increase by 6 dB per octave again in Region III. The critical frequency for the PC panel equals approximately 3200 Hz calculated by Eq. 2. The value of critical frequency is in the range of interest, which means the employed PC panels in the scale measurement showed their sound insulation performance not only in Region II but also in Region III. Recall from Figure 10 that in Region II below 3200 Hz the differences between the TLs and the predicted attenuations for the nearly-enclosed model were less than 10 dB, and in Region III the loss of TL caused by the coincident effect leads the TL much closer to the increased attenuation with increasing frequency. Once more, the further analysis based on the sound insulation theory proves that the PC panels employed in our test were not able to sufficiently insulate the

356 traffic noise.

357 From these findings we can summarize that the material with high density  
358 has a good sound insulation property due to the mass law. On the other hand,  
359 with high critical frequency the material shows its TL performance in the test  
360 almost in Region II to avoid the coincident effect. Hence it is better to select  
361 a kind of transparent material with high density, high critical frequency and  
362 high flexibility for the arched shape. According to this description, the 10-  
363 millimetre-thick rubber was chosen. The TL of the arched parts must be  
364 improved considerably by the heavy mass owing to the high thickness of  
365 rubber. Although the density can be expected to be between  $0.96 \text{ g/cm}^3$   
366 and  $1.3 \text{ g/cm}^3$  only as large as that for the PC panels, with a low Young's  
367 Modulus (0.001-0.0022 GPa) its critical frequency can be up to over 40 kHz so  
368 that its TL performs only by the mass law in the scale model measurement.  
369 Furthermore, it is quite easy to reshape. Thus, it was possible to reduce the  
370 differences between measured and predicted results by the rubber covering  
371 with no need to worry about the transparency of the material.

372 For the sake of comparison between the scale model with and without  
373 rubber, the rubber was only applied to coat the whole model of barrier, not  
374 to act as the alternative to any existing materials constructing the barrier.  
375 Figure 6(a) shows its application in our scale model measurement.

### 376 3.5. *Effect of rubber covering*

377 In order to improve the sound insulation, repeated scale tests with addi-  
378 tional 10-mm-thick rubber covering on the outer surface of the model were  
379 carried out. Figure 11 illustrates all the configurations of the tested mod-  
380 els with the rubber covering. The black parts represent the rubber coating  
381 on all the outer surfaces of the barrier. In addition, to test the effect to  
382 the nearly-enclosed barrier (Figure 11(d1)(d2)), a comparison for the double-  
383 straight barrier between the model with and without the rubber covering was  
384 made as well. Figure 12 compares the measured results with the correspond-  
385 ing BEM predictions for the double-straight model and the nearly-enclosed  
386 barrier, respectively. Identically to the previous observations, the measured  
387 results for the double-straight barrier with the rubber covering correspond to  
388 the 2.5-D BEM predictions, and the differences between the measured results  
389 and the predictions are a little smaller than those for the case without the  
390 rubber covering (Figure 9(a)). This proves the employed wood planks were  
391 sufficiently thick to insulate sound when the barrier shape was straight. And  
392 with the help of the rubber covering the improvement was negligible. Then

393 to compare with the nearly-enclosed barrier it is encouraging that with the  
 394 addition of the rubber covering the agreement between the measured and pre-  
 395 dicted results was obviously improved comparing with that shown in Figure  
 396 9(b) . This agreement provides very strong evidence that the employed PC  
 397 panels cannot be assumed to be totally reflective panels to preventing sound  
 398 from transmitting through when the barrier has a nearly-enclosed shape, and  
 399 adding a cover of material with good sound insulation to the surface of the  
 400 PC panels is a practicable way to improve the barrier attenuation, to bring  
 401 it close to the expectation of 2.5-D BEM model.

402 As a result, it can be concluded that generally there is good agreement  
 403 between the measured results obtained in the scale model with the rubber  
 404 covering and those predicted by the 2.5-D BEM model of the nearly-enclosed  
 405 barrier.

On the basis of the agreement between the measured results and predic-

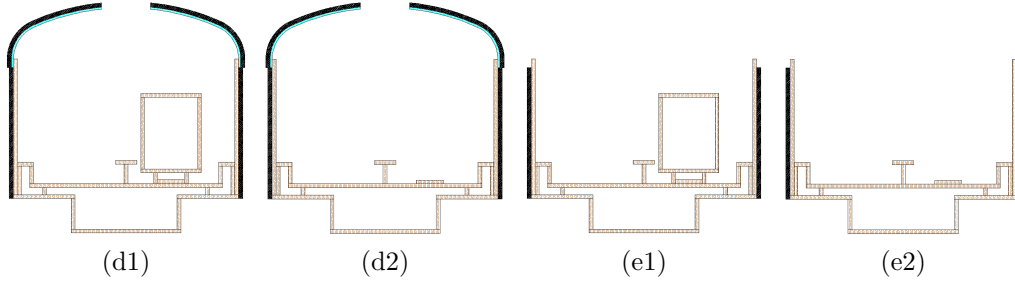
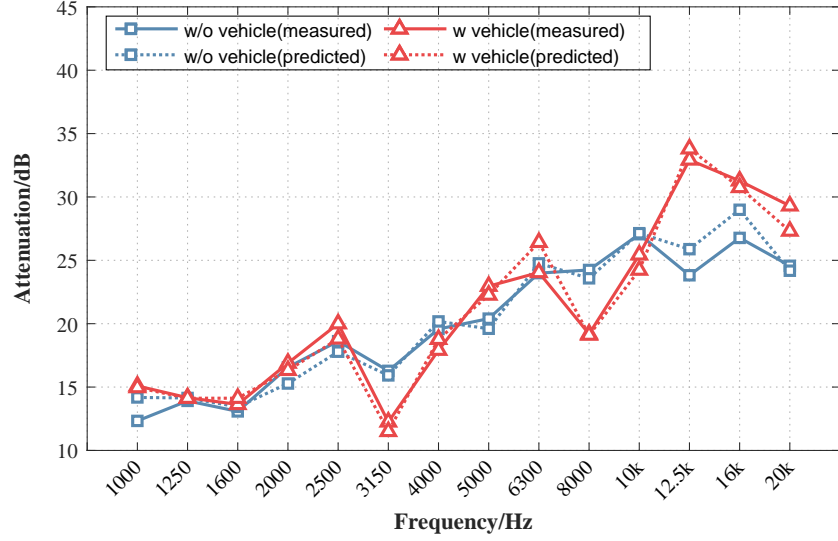


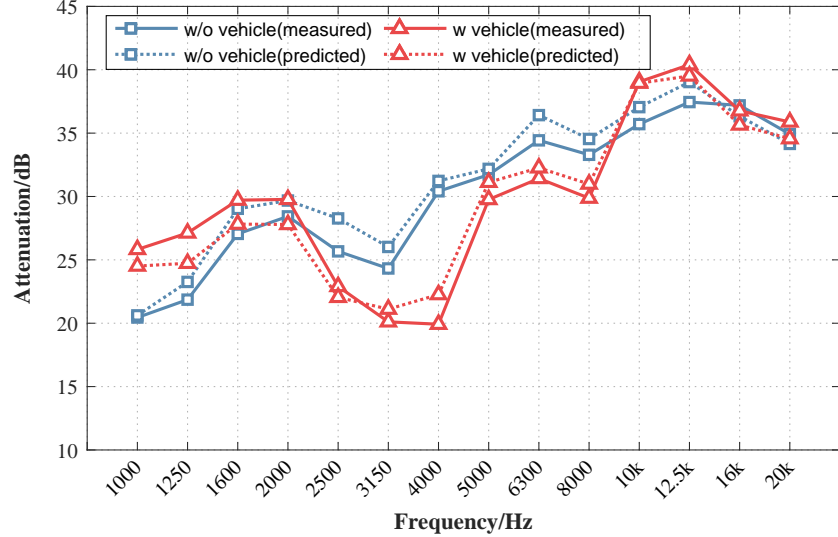
Figure 11: The configurations of the tested models with the rubber covering

406 tions for the nearly-enclosed barrier, the number effect of incoherent point  
 407 sources on the barrier attenuation was analyzed. In order to validate the  
 408 2.5-D BEM predictions with several incoherent point sources the number  
 409 of loudspeakers was changed as mentioned previously. Figure 13 provides  
 410 the information about the results for different numbers of incoherent point  
 411 sources for the nearly-enclosed barrier. Before the discussion on the number  
 412 effect of incoherent point sources, it is necessary as a starting point to verify  
 413 the predictions by the measured results. Apparently each comparison shows  
 414 good agreement, as our expectation. Then, we found that the curves in Fig-  
 415 ure 13 vary widely with increased frequency: some are extremely fluctuating,  
 416 while others tend to smooth.

418 In Figure 13, it is easy to understand the growth of attenuation fluctu-  
 419 ates seriously with frequency for one point source(blue curves). And yet it is



(a) Double-straight barrier on the viaduct

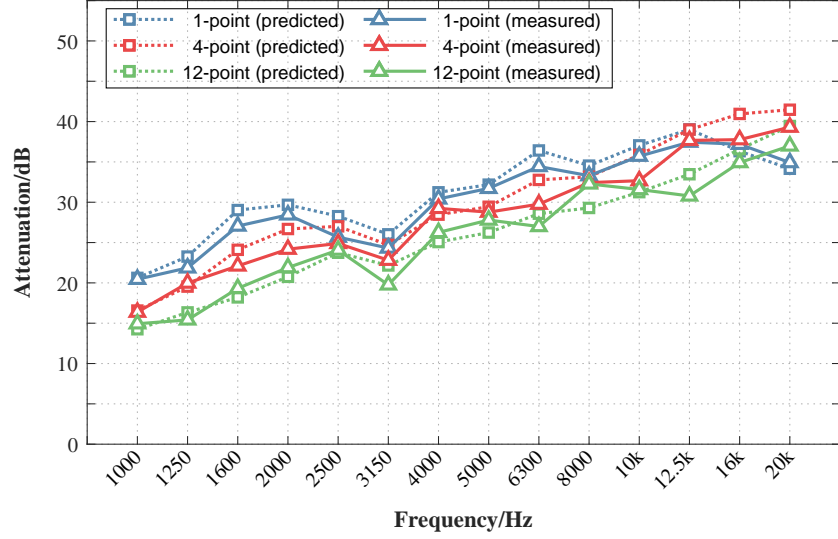


(b) Nearly-enclosed barrier on the viaduct

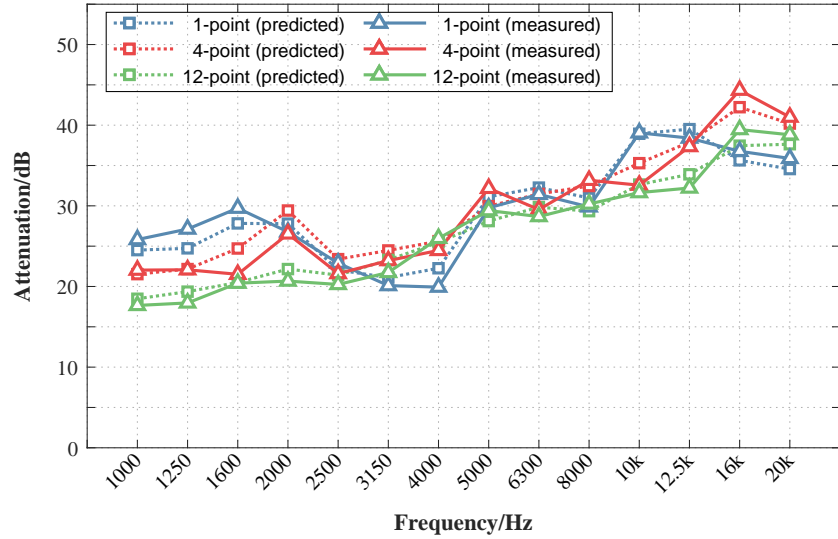
Figure 12: Measured and predicted attenuations for the model with the rubber covering(a) double-straight barrier(Figure 11(e1)(e2)); (b) nearly-enclosed barrier(Figure 11(d1)(d2))

420 interesting that the attenuation tends to increase smoothly as the number of  
 421 incoherent point sources increases to four(red curves). When increased to the  
 422 maximum number of sources(green curves), the attenuations have a visible  
 423 decline at each frequency band in comparison with those of four-point source.





(a) Without vehicle



(b) With vehicle

Figure 13: Measured and predicted attenuation for the nearly-enclosed barrier: (a) without vehicle(Figure 11(d2)); (b) with vehicle(Figure 11(d1))

424 In addition, the comparison of the results between the model with and with-  
 425 out the vehicle structures was also considered. The frequency-attenuation  
 426 curves with the vehicle structures(Figure 13(b)) fluctuate much more than

427 those without the vehicles(Figure 13(a)), even for the smoothest curves cor-  
428 responding to the twelve incoherent point sources. This is due to the multiple  
429 reflection between the vehicle structure and the inner surface of the barrier,  
430 which can be reduced by treating the inner surface with an absorbent mate-  
431 rial.

432 All the findings in the scale measurement for the nearly-enclosed model  
433 with a rubber covering demonstrate good agreement with those predicted by  
434 the 2.5-D BEM approach for each the third octave band from 1000 Hz to  
435 20 kHz. To summarize, it can be assumed that the acoustic performance of  
436 the nearly-enclosed barrier investigated by the 2.5-D BEM predictions for  
437 incoherent point sources are reliable.

## 438 4. 2.5-D BEM predictions

439 The 2.5-D BEM program was used to make predictions of attenuations  
440 reduced by the nearly-enclosed barrier in order to identify its acoustic per-  
441 formance in the surroundings. Run times with the complex geometry of  
442 the nearly-enclosed barrier and railway vehicle simulation were excessive. In  
443 order to reduce calculation times only the model with viaducts and nearly-  
444 enclosed barriers but without rubber coverings(Figure 7(a1)) was calculated  
445 for the whole frequency spectrum. Identically to the measurement, the cal-  
446 culation was also completed without barriers(Figure 7(c1)) for attenuation  
447 analysis.

### 448 4.1. *Rearrangement of source and receiver positions*

449 As we discussed in a previous article[21], based on the diffraction theory  
450 the receiver positions need to be in all six significant acoustic areas: bright  
451 zone, transition zone and shadow zone in the near field and far field, respec-  
452 tively. The bright zone and transition zone for the nearly-enclosed barrier  
453 were elongated and quite close to the source on the horizontal axis due to  
454 the special shape of its top. The rest is therefore the shadow zone covering  
455 most of the acoustic field. Considering that it is impossible to develop any  
456 construction projects at the two former zones, our observation in this sec-  
457 tion is focused on the performance at the shadow zone. Within this zone  
458 the receiver positions were in the near field and far field separately. For the  
459 frequency range of interest(50 Hz- 1000 Hz in the full scale) the boundary  
460 between the near field and far field is located at around 14 meters away  
461 from the source. Notice that further frequencies in Section 4 will be given

462 in the full scale. Consequently, by the grid-form method referred to in [21],  
 463 predictions were made at receivers placed at the four receiver distances(5,  
 464 10, 20 and 40 m from the centre of the track) on the horizontal axis and  
 465 at the three receiver heights(1.5 m above, 1.5 m below and at the height of  
 466 the track) on the vertical axis. Figure 14 illustrates these receiver positions.  
 467 Given the large number of receiver positions, it was important to assign a  
 468 name to each receiver. The name of each receiver begins with "M". The first  
 469 number represents the column number which is smaller as the receiver gets  
 470 closer to the source, whereas the second number represents the row number  
 471 which is larger as the receiver gets closer to the ground. A symbol like "M1-"  
 472 "M -1" which will be seen in later sections represents, for example, all the  
 473 receivers in the first column or the first row, respectively.

Unlike only one point source simulated on the cross-section of the scale

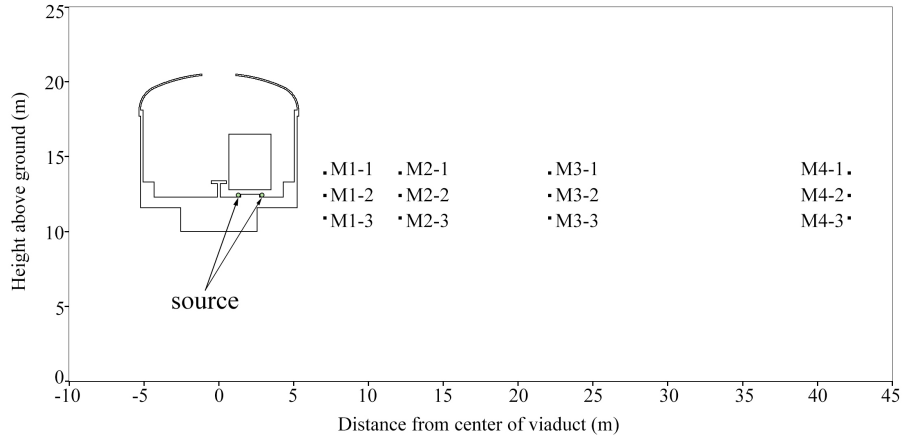


Figure 14: Source and receiver positions in the 2.5-D BEM calculation

474 model in the measurement, the noise sources were modelled as two incoher-  
 475 ent point sources on the cross-section positioned at the approximate height  
 476 of two rail-wheel interaction positions(represented by two dots in Figure 14).  
 477 Note that the source to receiver distance discussed below represents the dis-  
 478 tance horizontally away from centre of track(also the centre of two incoherent  
 479 point sources on the cross-section). Identically to the previous calculation,  
 480 the predictions for different numbers of sources(1, 4 and 12 incoherent point  
 481 sources arrayed along the length of barrier) were made as well for all the re-  
 482 ceivers mentioned above. Each distance perpendicular to the page between  
 483 the source and receiver is also the same as that in the previous calculations.  
 484

485 In the 2.5-D calculations, sound pressure was predicted for several in-  
486 dividual frequencies with a linear spacing of 0.1 Hz per third octave band  
487 ranging from 50 Hz to 1000 Hz. The energy for all the incoherent point  
488 sources in the model was summed within each band yielding the third octave  
489 band spectrum. Eventually the attenuation spectrum was calculated by the  
490 logarithmic ratio of the energy obtained between the model without and with  
491 the barrier.

#### 492 *4.2. Near field*

493 Figure 15&16 show the predicted attenuations for the receivers in the  
494 near field for different numbers of incoherent point sources. For the source to  
495 receiver distance of 5 m there is a consistent pattern in the results obtained,  
496 with the attenuation varying with the third-octave band for a given number  
497 of sources, but to different degrees as observed in Figure 15. Among them  
498 receiver M1-1 is the most greatly affected by changes in the band for a given  
499 number of sources while there is the least effect for M1-3. And it can be seen  
500 more obviously that the attenuation obtained with the highest receiver M1-1  
501 is significantly greater than that obtained with the lowest receiver M1-3 for  
502 all the third-octave bands of interest. That means the attenuation increases  
503 with the increased height of receivers for all the cases examined in M1- and  
504 the effect is very considerable.

505 However, with the increased number of sources, attenuation always de-  
506 creases for a given receiver, and more importantly, it tends to fluctuate less.  
507 Taking an example for receiver M1-1, the global maximum of attenuation for  
508 one-point source is 41.61 dB at 630 Hz, while there are two local maximums,  
509 31.94 dB and 28.56 dB at 250 Hz and 100 Hz, respectively. For the four-point  
510 source the increase of attenuation from 630 Hz, to 1000 Hz is positive but  
511 slow so that the global maximum is located at the maximum band of interest,  
512 i.e. 41.83 dB at 1000 Hz. And obviously there is only one local maximum:  
513 27.89 dB at 100 Hz. For the twelve-point source the attenuation increases  
514 smoothly with the increased band and therefore it is difficult to find a local  
515 maximum. Again, the global maximum is located at the maximum band of  
516 interest, i.e. 39.34 dB at 1000 Hz.

517 The attenuation for the source to receiver distance of 5 meters in general  
518 is higher than 13 dB for each band, and from 400 Hz to 1000 Hz it is even  
519 higher than 20 dB. While for the source to receiver distance of 10 m the  
520 attenuation is on average higher than 10 dB, and from 400 Hz to 1000 Hz it  
521 is even higher than 15 dB. Figure 16 shows the attenuation achieved for the

source to barrier distance of 10 m for all configurations examined. Again, it can be observed that there is a similar pattern in the results obtained with the attenuation varying with the third-octave band for a given number of source. However, unlike the predictions for receiver in M1- the attenuations for the receiver in M2- are not greatly affected by changes in the height of the receiver for a given third-octave band ranging from 50 Hz to 400 Hz, although there is a small effect on attenuation from 500 Hz to 1000 Hz.

For the source to receiver distance of 10 m with the increased number of source attenuation decreases again and tends to fluctuate less for a give receiver. There is a similar trend for each receiver in M2- that the attenuation ranging from 400 Hz to 1000 Hz firstly increases and then decreases for one-point source, then increases slowly when the number increases to four, and finally increases linearly for the twelve-point source. Because of this, the associated frequency of the global maximum increases with the increased number of sources, i.e. the global maximum for M2-1 is 25.33 dB, 28.13 dB and 27.2 dB at 630 Hz, 800 Hz and 1000 Hz for the one-point, four-point and twelve-point source respectively. On the other hand the global minimum of attenuation for the one-point source for the receiver in M2- can be seen clearly at 160 Hz with the value of approximately 6 dB, and it is the most distinct trough in Figure 16. Nevertheless, this trough gradually disappears for the four-point and twelve-point sources.

The following general conclusions can be drawn from the above: first, the attenuation with an average of approximately 15 dB can be achieved in the near field; secondly, the height effect of the receiver on attenuation is significant for the source to receiver distance of 5 m while that for the source-receiver distance of 10 m is almost invisible; thirdly, the increased number of source can result in the smoother and lower attenuation.

#### 4.3. Far field

Figure 17 &18 show the predicted attenuations for the receivers in the far field for different numbers of incoherent point sources. For the source to receiver distance of 20 m there is again a similar trend in the results obtained, with the attenuation varying with the third-octave band for the whole frequency range for a given number of sources(as observed in Figure 17). However, an opposite trend for the height effect of receivers can be observed in M3- that attenuation decreases with the increased height of receivers for a given number of sources but the effect is very small.

559 With the increased number of sources, attenuation decreases for a given  
560 receiver. A similar noticeable trough can be observed at 160 Hz in Figure 17  
561 for one-point source, but it is surprising that it is a negative value and its  
562 magnitude increases with decreased height for the receiver in M3- with the  
563 lowest value of -2.46 dB. However, for all cases of the other two source types  
564 the magnitudes of attenuations are always positive since the attenuation is  
565 more stable with smaller fluctuations. For a given receiver there is also a  
566 peak at 250 Hz for the one-point source but less obviously for the four-point  
567 source, and it finally disappears for the twelve-point source. The attenuation  
568 for the twelve-point source for the receiver in M3- fluctuates within a small  
569 range of 6-13 dB ranging from 50 Hz to 400 Hz, and it increases slowly from  
570 400 Hz to 1000 Hz.

571 The attenuation for the source to receiver distance of 20 m average is  
572 lower than 20 dB for each band, while for the source to receiver distance  
573 of 40 m the attenuation is on average lower than 10 dB. Figure 18 shows  
574 the attenuation achieved for the source to barrier distance of 40 m for all  
575 configurations examined. Again, it can be observed that there is a similar  
576 pattern in the results obtained, with the attenuation varying with the third-  
577 octave band for a given number of sources. And similar to those in Figure  
578 17 attenuation decreases with the increased height of the receiver for a given  
579 number of sources, but the effect is quite small.

580 Unlike the negative value of global minimum for all the receivers in M3-  
581 for the one-point source, there is a negative attenuation as the global min-  
582 imum only at 160 Hz for M4-2 for the one-point and the four-point source.  
583 Apart from that, for the source to receiver distance of 40 m with increased  
584 number of sources, attenuation for the receiver in M4- decreases and fluctu-  
585 ates less again for a give receiver. For the global maximum, the associated  
586 frequency is unchanged with the value of 50 Hz. And the magnitude firstly  
587 increases and then decreases with increasing number of sources, i.e. for M4-  
588 1 it is 17.80 dB, 18.58 dB and 16.10 dB for the one-point, four-point and  
589 twelve-point source, respectively.

590 The following general conclusions can be drawn from the above: first,  
591 the attenuation with an average of approximately 10 dB can be achieved in  
592 the far field; secondly, the performance in the far field reduces with increasing  
593 height of receivers but the effect is very small, in other words, the perfor-  
594 mance is relatively unaffected by the height of receivers; thirdly, the increased  
595 number of sources can result in the attenuation being much smoother and  
596 lower, especially eliminating the negative value induced by the small number

597 of sources.

## 598 5. Discussion and conclusions

599 The 2.5-D BEM program developed for incoherent point source calculations was used to solve the practical problem of assessing the acoustic performance outside a nearly-enclosed barrier with infinite length. The results of a preliminary investigation calculated by the 2.5-D BEM program showed that there were amounts of peaks in the frequency domain of sound pressure in the surroundings of the nearly-enclosed barrier. With good agreement between the sound pressure distributions at the peak frequencies and the corresponding acoustic modes of the air cavity inside the barrier, a reasonable explanation of these peaks was given that when the shape of the barrier was nearly-enclosed, the acoustic resonance effect generated by the open air cavity could result in extremely high levels at the resonance frequencies, directly deteriorating the barrier performance. To suppress the resonance effect the additional absorptive treatments on the inner surface of the barrier is proposed for further research.

613 To validate the predictions a series of scale model measurements were made since the scale modelling technique allowed the effect of the employed material on the barrier performance to be more realistic. It was shown from the comparison that there was a significant deviation between the measured and predicted results for the nearly-enclosed barrier, but good agreement for the double-straight barrier. Measured attenuations for the nearly-enclosed barrier were obviously higher than those for the double-straight type in the mid-frequency range, while at high frequencies, attenuations for the nearly-enclosed barrier were almost the same as those for the double-straight type. More importantly, the measured results for the nearly-enclosed barrier were much lower than those predicted by the BEM, which may result from the insufficient sound insulation of the PC panels.

625 Based on the sound insulation theory and the measured TLs in [19], the transmission loss of the 5-mm-thick PC panels employed in the scale model was estimated. The comparisons show that the predicted attenuations for the nearly-enclosed type were quite close to the transmission loss of the PC panels in the frequency range of interest. According to the calculation of barrier attenuation in the form of energy transfer, the correction for sound transmission could not be ignored. Therefore, the insufficient sound insulation of the PC panels was identified to be the main cause of the differences

633 between the measured and predicted attenuations for the nearly-enclosed  
634 barrier. As mentioned above, the PC panels, employed for the arched parts  
635 in the full-scale prototype of the nearly-enclosed barrier in China, have a  
636 thickness of only 6.5 mm, a little thicker than those employed in the scale  
637 model in our test. Thus, the sound insulation of the PC panels in the actual  
638 project are considered to be not sufficient as well. The need for transparent  
639 material with better sound insulation and high flexibility was long ignored  
640 and urgent for the arched parts, both in the scale model tests and the actual  
641 projects.

642 With the help of 10-mm-thick rubber, a supplementary measurement was  
643 developed for solving the difficulty. Fortunately, the predictions of one-third  
644 octave band levels using the 2.5-D BEM program were shown to be com-  
645 parable with the 1:20 scale measurements by fully coating all surfaces with  
646 rubber so that confidence can be given in the BEM predictions for the whole  
647 field. The compared results also reconfirmed the insulation problem of the  
648 PC panels for the nearly-enclosed barrier. In addition, the predictions for the  
649 four-point and twelve-point sources were shown to be comparable with the  
650 measured results, which provides us the opportunity to discuss the number  
651 effect of incoherent point sources.

652 Considering the complex sound field distribution caused by the specific  
653 structure of a nearly-enclosed barrier, in order to understand thoroughly  
654 the barrier performance, the receiver positions were rearranged according to  
655 [21]. The rearrangement approach based on the diffraction theory was used  
656 to estimate the performance of the sound barrier in each area with different  
657 acoustic features.

658 As expected, the attenuation of the nearly-enclosed barrier averaged around  
659 15 dB in the near field and around 10 dB in the far field. This indicates that  
660 the nearly-enclosed type has a more effective and efficient performance on the  
661 premise that all the boundaries are acoustically rigid. This kind of barrier  
662 with high attenuation designed by the modification of shape requires the em-  
663 ployed material with sufficiently high sound insulation property. Otherwise  
664 the design will be largely failed and not economical for the practical use.

665 It was also shown that the attenuation decreased with increasing source-  
666 receiver distance, while it increased with increasing height of receivers only  
667 in the column which was the closest to the source in our study. For the  
668 other three source-receiver distances the height effect of receiver was almost  
669 negligible. The number effect of incoherent point sources was also taken into  
670 account for modelling railway traffic noise. Apparently, the increased num-

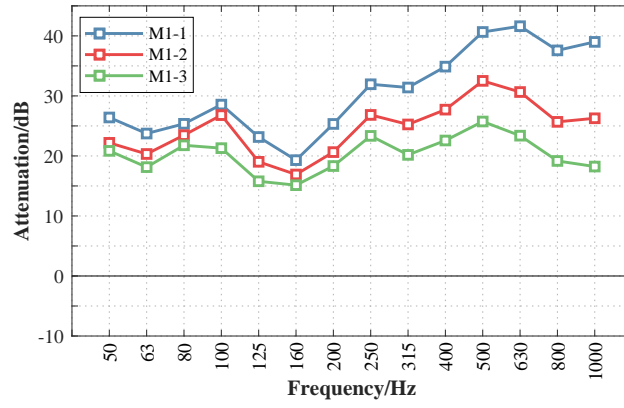


ber of source can result in much smoother and lower attenuations for all the areas, especially eliminating the negative value induced by the small number of sources. In addition, the resonance effect referred to previously can be the reasonable explanation of the negative values of the attenuations in the far field.

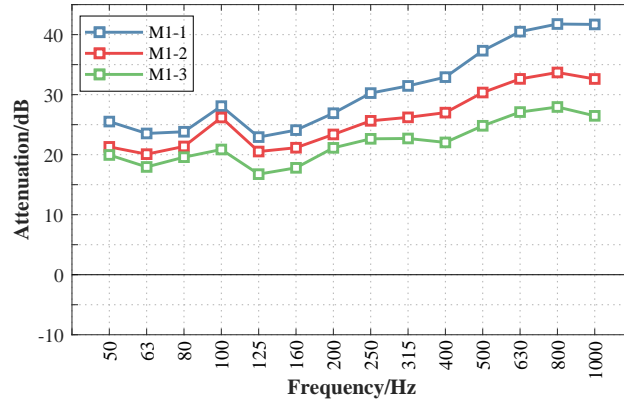
- [1] A. Jolibois, J. Defrance, H. Koreneff, P. Jean, D. Duhamel, V. Sparrow, In situ measurement of the acoustic performance of a full scale tramway low height noise barrier prototype, *Applied Acoustics* 94 (2015) 57–68 (2015). doi:10.1016/j.apacoust.2015.02.006. URL <http://dx.doi.org/10.1016/j.apacoust.2015.02.006>
- [2] X. LI, D. Yang, W. GAO, Y. LUO, Study on Vibration and Noise Reduction of Semi- or Fully- Enclosed Noise Barriers of High Speed Railways, *Noise and vibration control* 38 (Z1) (2018). doi:10.3969/j.issn.1006-1355.2018.Z1.002.
- [3] G. R. Watts, D. C. Hothersall, K. V. Horoshenkov, Measured and predicted acoustic performance of vertically louvred noise barriers, *Applied Acoustics* 62 (11) (2001) 1287–1311 (2001). doi:10.1016/S0003-682X(00)00101-8.
- [4] G. R. Watts, Acoustic performance of parallel traffic noise barriers, *Applied Acoustics* (1996). doi:10.1016/0003-682X(95)00031-4.
- [5] D. J. Oldham, C. A. Egan, A parametric investigation of the performance of multiple edge highway noise barriers and proposals for design guidance, *Applied Acoustics* (2015). doi:10.1016/j.apacoust.2015.03.012.
- [6] C. Yang, J. Pan, L. Cheng, A mechanism study of sound wave-trapping barriers 134 (3) (2013). doi:10.1121/1.4816542.
- [7] W. Bowlby, L. F. Cohn, A model for insertion loss degradation for parallel highway noise barriers, *The Journal of the Acoustical Society of America* 80 (3) (2005) 855–868 (2005). doi:10.1121/1.393909.
- [8] M. R. Monazzam, S. M. B. Fard, Impacts of Different Median Barrier Shapes on a Roadside Environmental Noise Screen, *Environmental Engineering Science* (2011). doi:10.1089/ees.2010.0269.

- 703 [9] G. R. Watts, N. S. Godfrey, Effects on roadside noise levels of  
704 sound absorptive materials in noise barriers, *Applied Acoustics* (1999).  
705 doi:10.1016/S0003-682X(99)00007-9.
- 706 [10] S. Kirkup, *The BEM in Acoustics* (1998) 161 (1998).
- 707 [11] A. Muradali, K. Fyfe, A study of 2D and 3D barrier insertion loss using  
708 improved diffraction-based methods, *Applied Acoustics* 53 (1-3) (2002)  
709 49–75 (2002). doi:10.1016/s0003-682x(97)00040-6.
- 710 [12] P. Jean, A variational approach for the study of outdoor sound propa-  
711 gation and application to railway noise, *Journal of Sound and Vibration*  
712 (1998). doi:10.1006/jsvi.1997.1407.
- 713 [13] R. Seznec, Diffraction of sound around barriers: Use of the bound-  
714 ary elements technique, *Topics in Catalysis* (1980). doi:10.1016/0022-  
715 460X(80)90689-6.
- 716 [14] D. Duhamel, Efficient calculation of the three-dimensional sound pres-  
717 sure field around a noise barrier, *Journal of Sound and Vibration* 197 (5)  
718 (1996) 547–571 (1996). doi:10.1006/jsvi.1996.0548.
- 719 [15] P. Jean, J. Defrance, Y. Gabillet, The importance of source type on the  
720 assessment of noise barriers, *Journal of Sound and Vibration* 226 (2)  
721 (1999) 201–216 (1999). doi:10.1006/jsvi.1999.2273.
- 722 [16] R. Makarewicz, J. Jarz, A. Preis, Rail Transportation Noise With and  
723 Without a Barrier, *Applied Acoustics* 26 (July 1988) (1989) 135–147  
724 (1989).
- 725 [17] R. Bialecki, R. Dallner, G. Kunhn, Minimum distance calculation be-  
726 tween a source point and a boundary element, *Engineering Analysis with*  
727 *Boundary Elements* 12 (1993) (1994) 211–218 (1994).
- 728 [18] J. Zhao, X. M. Wang, J. M. Chang, Y. Yao, Q. Cui, Sound insulation  
729 property of wood-waste tire rubber composite, *Composites Science and*  
730 *Technology* (2010). doi:10.1016/j.compscitech.2010.03.015.
- 731 [19] J. H. Lee, J.-R. Park, W.-M. Lee, J.-H. Son, I.-H. Kim, K. S.  
732 Kim, Sound Insulation Properties of Polymer Soundproof Pan-  
733 els, *Journal of Korean Society of Environmental Engineers* (2014).  
734 doi:10.4491/ksee.2013.35.8.592.

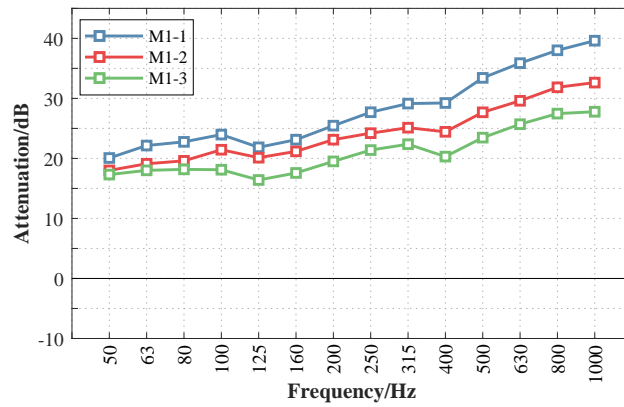
- 735 [20] Y. Yang, B. Li, Z. Chen, N. Sui, Z. Chen, M. U. Saeed, Y. Li,  
736 R. Fu, C. Wu, Y. Jing, Acoustic properties of glass fiber assembly-filled  
737 honeycomb sandwich panels, *Composites Part B: Engineering* (2016).  
738 doi:10.1016/j.compositesb.2016.04.046.
- 739 [21] Q. Li, D. Denis, Y. Luo, H. Yin, Improved Methods for In-situ Mea-  
740 surement Railway Noise Barrier Insertion Loss, *Transactions of Nanjing*  
741 *University of Aeronautics and Astronautics* (2018).



(a) one-point source

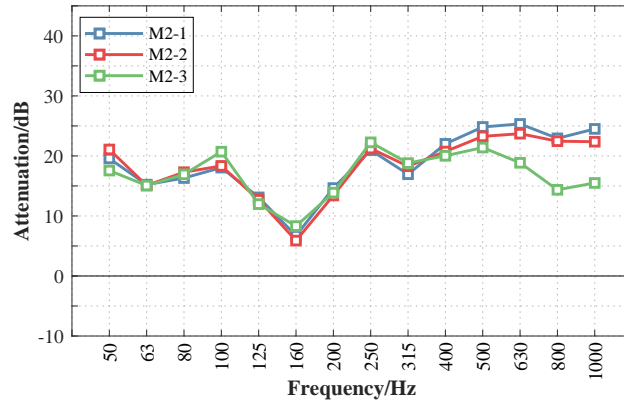


(b) four-point source

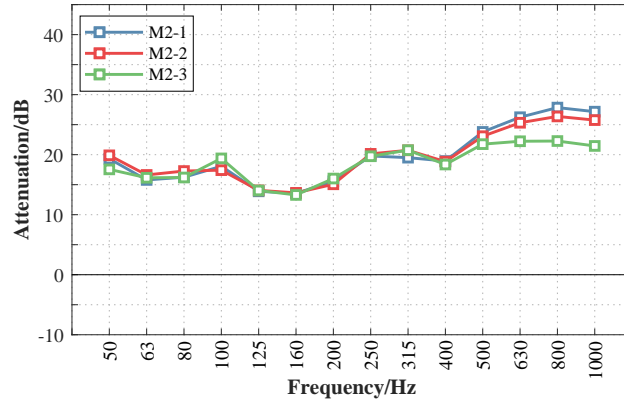


(c) twelve-point source

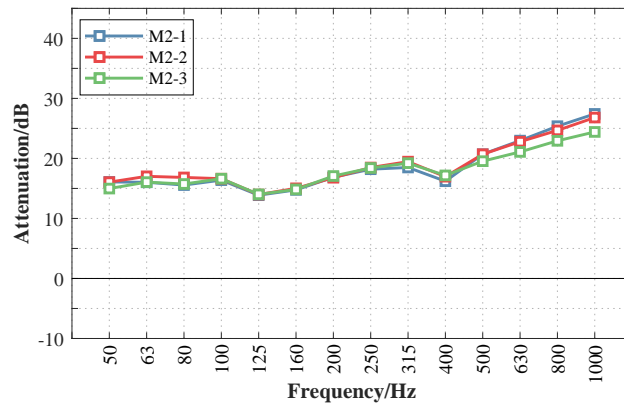
Figure 15: Predicted attenuations for the source to receiver distance of 5 meters



(a) one-point source

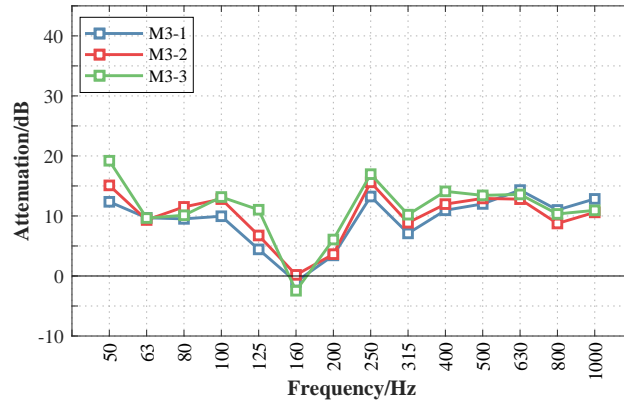


(b) four-point source

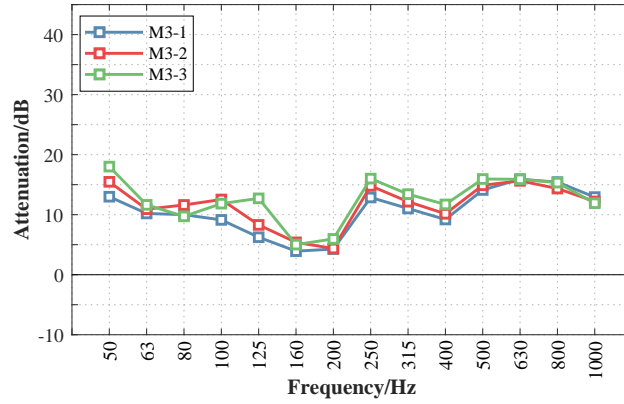


(c) twelve-point source

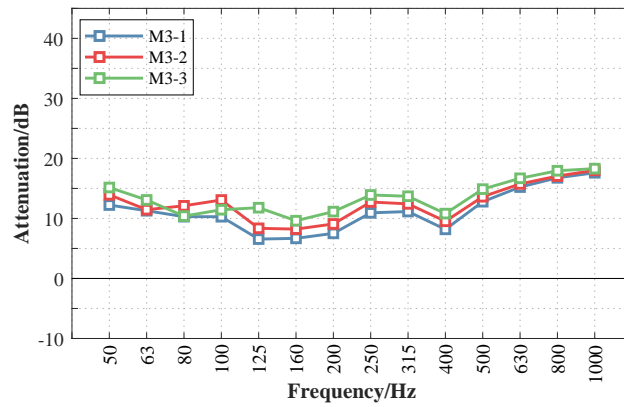
Figure 16: Predicted attenuations for the source to receiver distance of 10 meters



(a) one-point source

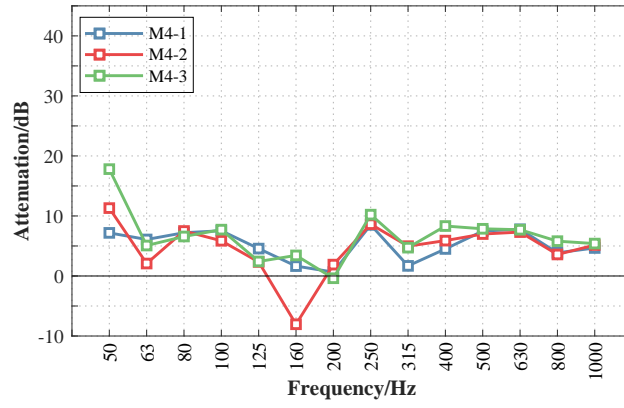


(b) four-point source

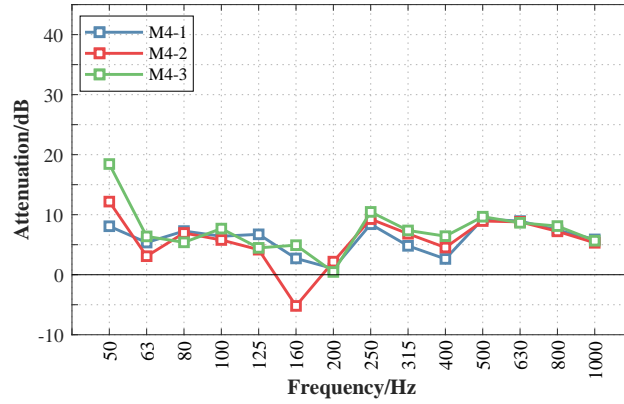


(c) twelve-point source

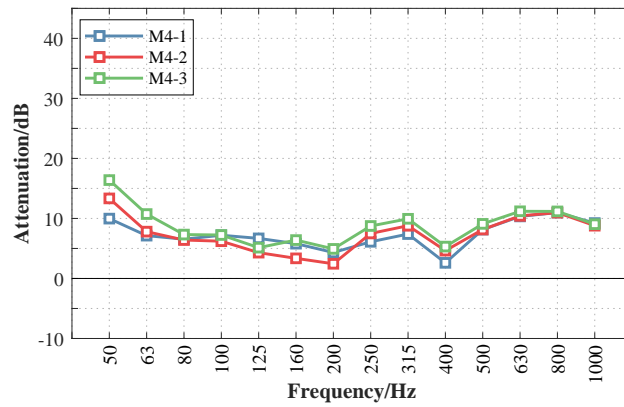
Figure 17: Predicted attenuations for the source to receiver distance of 20 meters



(a) one-point source



(b) four-point source



(c) twelve-point source

Figure 18: Predicted attenuations for the source to receiver distance of 40 meters